Original Article

Detection of chronic obstructive pulmonary disease with deep learning using inspiratory and expiratory chest computed tomography and clinical information

Zhuoneng Zhang[1#^], Fan Wu[2,3#^], Yumin Zhou[2,3#^], Donglin Yu[1], Chuanqi Sun[1], Xiangyu Xiong[1], Zhiquan Situ[1], Zeping Liu[1], Anyan Gu[1], Xin Huang[1], Youlan Zheng[2], Zhishan Deng[2^], Ningning Zhao[2^], Zhaowei Rong[1], Ji He[1], Guoxi Xie[1], Pixin Ran[2,3^]

[1]School of Biomedical Engineering, Guangzhou Medical University, Guangzhou, China; [2]Guangzhou Institute of Respiratory Health & State Key Laboratory of Respiratory Disease & National Center for Respiratory Medicine & National Clinical Research Center for Respiratory Disease, The First Affiliated Hospital of Guangzhou Medical University, Guangzhou, China; [3]Guangzhou National Laboratory, Guangzhou, China

Contributions: (I) Conception and design: F Wu, Z Zhang, Y Zhou, G Xie, P Ran; (II) Administrative support: Y Zhou, G Xie, P Ran; (III) Provision of study materials or patients: F Wu, Y Zhou, Y Zheng, Z Deng, N Zhao, P Ran; (IV) Collection and assembly of data: F Wu, Y Zhou, Y Zheng, Z Deng, N Zhao, P Ran; (V) Data analysis and interpretation: All authors; (VI) Manuscript writing: All authors; (VII) Final approval of manuscript: All authors.

[#]These authors contributed equally to this work.

Correspondence to: Pixin Ran, MD, PhD. Guangzhou National Laboratory, Guangzhou, China; Guangzhou Institute of Respiratory Health & State Key Laboratory of Respiratory Disease & National Center for Respiratory Medicine & National Clinical Research Center for Respiratory Disease, The First Affiliated Hospital of Guangzhou Medical University, No. 9 Huanbei Road, Haizhu District, Guangzhou 510120, China. Email: pxran@gzhmu.edu.cn; Guoxi Xie, PhD; Ji He, PhD. School of Biomedical Engineering, Guangzhou Medical University, No. 1 Xinzao Road, Panyu District, Guangzhou 511436, China. Email: guoxixie@163.com; heji@gzhmu.edu.cn.

Background: In recent years, more and more patients with chronic obstructive pulmonary disease (COPD) have remained undiagnosed despite having undergone medical examination. This study aimed to develop a convolutional neural network (CNN) model for automatically detecting COPD using double-phase (inspiratory and expiratory) chest computed tomography (CT) images and clinical information.

Methods: A total of 2,047 participants, including never-smokers, ex-smokers, and current smokers, were prospectively recruited from three hospitals. The double-phase CT images and clinical information of each participant were collected for training the proposed CNN model which integrated a sequence of residual feature extracting blocks network (RFEBNet) for extracting CT image features and a fully connected feed-forward network (FCNet) for extracting clinical features. In addition, the RFEBNet utilizing double- or single-phase CT images and the FCNet using clinical information were conducted for comparison.

Results: The proposed CNN model, which utilized double-phase CT images and clinical information, outperformed other models in detecting COPD with an area under the receiver operating characteristic curve (AUC) of 0.930 [95% confidence interval (CI): 0.913–0.951] on an internal test set (n=307). The AUC was higher than the RFEBNet using double-phase CT images (AUC =0.912, 95% CI: 0.891–0.932), single inspiratory CT images (AUC =0.888, 95% CI: 0.863–0.915), single expiratory CT images (AUC =0.897, 95% CI: 0.874–0.925), and FCNet using clinical information (AUC =0.805, 95% CI: 0.777–0.841). The proposed model also achieved the best performance on an external test (n=516) with an AUC of 0.896 (95% CI: 0.871–0.931).

Conclusions: The proposed CNN model using double-phase CT images and clinical information can automatically detect COPD with high accuracy.

^ ORCID: Zhuoneng Zhang, 0000-0002-0046-0985; Fan Wu, 0000-0003-0720-4674; Yumin Zhou, 0000-0002-0555-8391; Zhishan Deng, 0000-0003-3652-5493; Ningning Zhao, 0000-0003-3515-2445; Pixin Ran, 0000-0001-6651-634X.

Keywords: Chronic obstructive pulmonary disease (COPD); inspiratory; expiratory; double-phase; convolutional neural network (CNN)

Submitted Mar 25, 2024. Accepted for publication Aug 02, 2024. Published online Sep 26, 2024.
doi: 10.21037/jtd-24-367
View this article at: https://dx.doi.org/10.21037/jtd-24-367

Introduction

Chronic obstructive pulmonary disease (COPD) is a highly prevalent and heterogeneous disease characterized by airway obstruction, inflammation, and emphysema (1). It has become a major public health issue and is listed as the third leading cause of death by the World Health Organization (2). The identification of COPD typically relies on a pulmonary function test (PFT) which determines the forced expiratory volume in 1 second (FEV_1)/forced vital capacity (FVC) ratio to determine if it is less than 0.70 (1). However, the PFT requires strict training and quality control, and it is unable to directly observe lung structure. Compared to PFT, computed tomography (CT) is a more widely used disease inspection device, which can be used to quantitatively assess pulmonary structural abnormalities found in COPD patients. Nonetheless, some COPD patients lack significant textural symptoms on CT images, resulting in difficulty in detecting COPD through visual evaluation using CT images (3). Therefore, a convenient and accurate automatic strategy for detecting COPD based on CT images is imperative.

CT has been widely adopted for decades in routine screening to assess patients with pulmonary nodules and lung cancer (4-6). In recent years, several automatic detection methods based on chest CT have been proposed for diagnosing lung diseases, especially for detecting COPD (7-13). For example, González *et al.* proposed a convolutional neural network (CNN) model to achieve a COPD detection accuracy of 0.773 using four canonical CT slices, which were obtained at predefined anatomic landmarks in the CT volume (7); Tang *et al.* conducted a proof-of-concept study to examine the use of deep residual networks for COPD detection and achieved an area under the receiver operating characteristic (ROC) curve (AUC) of 0.889 (8); Ho *et al.* introduced a COPD grouping method based on deep learning (DL) and a parametric response mapping technique, which achieved a classification accuracy of 0.893 (9); Sun *et al.* proposed a weekly supervised DL approach for COPD detection, which obtained an AUC of 0.934 for an internal and 0.866 for an external test set (10). Although these methods have shown promising results, they only consider the images obtained from a single inspiratory CT, ignoring the potential benefits of expiratory CT images (14). Gawlitza *et al.* found that incorporating expiratory CT imaging can enhance the correlation between quantified CT parameters and lung function parameters, thereby improving the discriminative performance of different subtypes of COPD using quantified CT (15). Hasenstab *et al.* developed a DL algorithm using both inspiratory and expiratory CT to stage COPD severity by quantifying emphysema and air trapping on CT images (16).

In addition, patient clinical information is often essential in achieving a final diagnosis of COPD, including such items as age, sex, smoking status, respiratory symptoms, COPD assessment test (CAT), and clinical COPD questionnaire (CCQ) (17,18). However, few works have focused on improving the detection of COPD by fully exploring the

Highlight box

Key findings

- The proposed convolutional neural network (CNN) model using double-phase chest computed tomography (CT) images and clinical information can automatically detect chronic obstructive pulmonary disease (COPD) with high accuracy.

What is known and what is new?

- CT has been widely adopted for decades in routine screening to assess patients with pulmonary nodules and lung cancer. In recent years, several automatic detection methods based on chest CT have been proposed for diagnosing COPD.
- In this study, we developed a novel CNN model that integrates double-phase CT images and clinical information to improve the accuracy of COPD detection. It achieved the highest area under the receiver operating characteristic curve in the internal test set, and its generalizability was validated by the external test set.

What is the implication, and what should change now?

- Our findings suggest that the proposed model has the potential to be used as an automatic screening tool for identifying COPD patients in clinical practice.

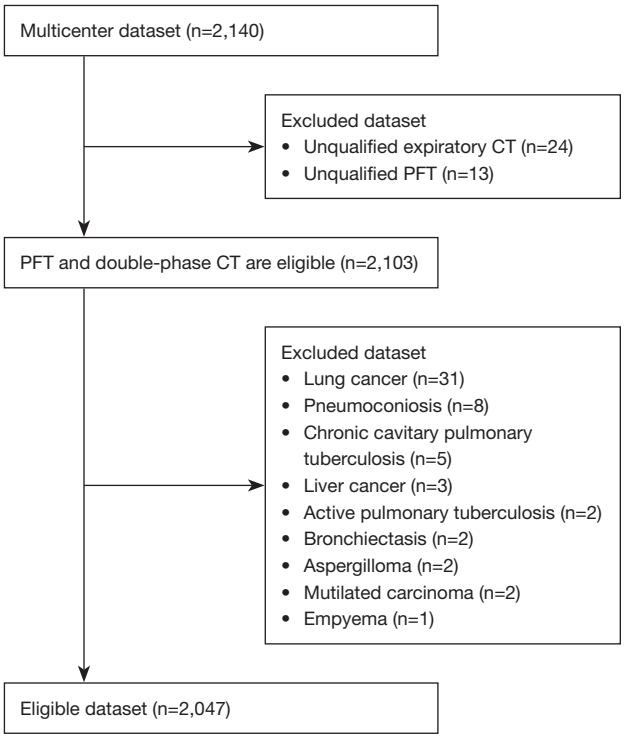

Figure 1 Flow diagram of participants inclusion. CT, computed tomography; PFT, pulmonary function test.

features on both inspiratory- and expiratory-phase (double-phase) CT and clinical information. Therefore, we propose a novel CNN model to automatically diagnose COPD by using double-phase chest CT images with clinical information. We present this article in accordance with the TRIPOD reporting checklist (available at https://jtd.amegroups.com/article/view/10.21037/jtd-24-367/rc).

Methods

Data acquisition

This is a prospective cohort study of which the data were collected from three hospitals. The study was conducted in accordance with the Declaration of Helsinki (as revised in 2013). The study was approved by the Ethics Board of The First Affiliated Hospital of Guangzhou Medical University (No. 2018-53), and informed consent was provided by all individual participants. The participant inclusion criteria of the study were as follows: (I) aged 40–80 years; (II) participants who are willing to participate in the study and provide a signed informed consent form; and (III) participants who complete PFT and double-phase chest CT scan (imaging at full inspiration and full expiration). The exclusion criteria were as follows: (I) lung cancer; (II) pneumoconiosis; (III) chronic cavitary pulmonary tuberculosis; (IV) liver cancer; and (V) history of other lung diseases except for asthma (e.g., active pulmonary tuberculosis, pneumoconiosis, extensive bronchiectasis, pulmonary aspergillosis).

According to the inclusion and exclusion criteria, a total of 2,047 participants were enrolled in the final analysis (see *Figure 1*). In addition, all participants underwent a clinical information questionnaire consisting of relevant factors such as sex, age, smoking status (never-smokers, ex-smokers, and current smokers), chronic respiratory symptoms (cough, expectoration, dyspnea, and wheezing), CAT, and CCQ. All participants (n=1,531) collected from two of the three hospitals using a United-Imaging scanner (United Imaging Healthcare, Shanghai, China) were denoted as Dataset A. All participants (n=516) collected from the other hospital using a Siemens scanner (Siemens Healthcare, Erlangen, Germany) were denoted as Dataset B. Detailed patient characteristics of the two datasets are shown in *Table 1* and detailed scan parameters are shown in *Table 2*. According to the data dividing rule of DL, the data in Dataset A were randomly divided into a training (n=1,224) and an internal testing set (n=307), and the data in Dataset B were used as an external test set.

COPD diagnosis was confirmed by an FEV_1 to FVC ratio of less than 0.70 after inhalation of a bronchodilator and the severity of COPD was staged by the Global Initiative for Chronic Obstructive Lung Disease (GOLD) standard.

Data processing

Inspired by previous study, we adopted an object detector to automatically select four representative canonical CT slices, including an axial slice at mitral valve, a coronal slice at ascending aorta, and two sagittal slices at right and left hila at preselected anatomic landmarks from an entire CT volume of each participant (19). Then, each representative CT slice was normalized to a standard lung window (i.e., window level: –400, window width: 1,400) to the grey value [0, 1] and down sampled to the size of 256×256 by a bilinear interpolation method to reduce the size of the image (20). Finally, the four preselected CT slices from inspiratory CT volume and those from expiratory CT volume of each participant were joined to an image with size of 2×512×512 which serves as input for the model. Thus, the input image

Table 1 Patient's characteristics of Dataset A and Dataset B, respectively

Variables	Dataset A (n=1,531)		Dataset B (n=516)	
	COPD (n=539)	Non-COPD (n=992)	COPD (n=369)	Non-COPD (n=147)
Men, n (%)	483 (89.6)	588 (59.3)	342 (92.7)	82 (55.8)
Age (years), mean ± SD	64.1±7.3	58.4±7.9	65.5±6.9	59.4±7.9
Smoking status, n (%)				
Never-smokers	86 (16.0)	525 (52.9)	42 (11.4)	85 (57.8)
Ex-smokers	149 (27.6)	126 (12.7)	125 (33.9)	24 (16.3)
Current smokers	304 (56.4)	341 (34.4)	202 (54.7)	38 (25.9)
Respiratory symptoms, n (%)				
Cough	179 (33.2)	121 (12.2)	190 (51.5)	33 (22.4)
Expectoration	240 (44.5)	204 (20.6)	208 (56.4)	42 (28.6)
Dyspnea	214 (39.7)	211 (21.3)	171 (46.3)	42 (28.6)
Wheezing	100 (18.6)	102 (10.3)	75 (20.3)	17 (11.6)
CCQ, mean ± SD	0.5±0.6	0.3±0.4	0.8±0.7	0.5±0.7
CAT, mean ± SD	4.3±4.9	2.9±3.7	6.3±5.6	4.4±5.6
FEV_1 (L), mean ± SD	1.98±0.62	2.42±0.56	1.92±0.57	2.38±0.59
FVC (L), mean ± SD	3.29±0.77	3.07±0.74	3.38±0.77	3.06±0.77
FEV_1/FVC, mean ± SD	59.3±10.5	79.1±6.3	56.4±9.0	78.4±5.2
FEV1% predicted, mean ± SD	74.6±21.4	96.5±15.1	74.2±18.2	98.5±14.1
GOLD stage, n (%)				
GOLD 1	242 (44.9)	NA	147 (39.8)	NA
GOLD 2	218 (40.4)	NA	189 (51.2)	NA
GOLD 3	64 (11.9)	NA	30 (8.1)	NA
GOLD 4	15 (2.8)	NA	3 (0.8)	NA

Dataset A contains all participants from two of the three hospitals and Dataset B contains those from the other hospital. COPD, chronic obstructive pulmonary disease; SD, standard deviation; CCQ, clinical COPD questionnaire; CAT, COPD assessment test; FEV_1, forced expiratory volume in one second; FVC, forced vital capacity; GOLD, Global Initiative for Chronic Obstructive Lung Disease; NA, not applicable.

Table 2 Detailed CT scan parameters

Parameters	United-Imaging	Siemens
Scan model	uCT 760	Definition AS Plus
Scan type	Spiral	Spiral
Scan region	Lungs	Lungs
Rotate time (s)	0.5	0.5
Tube voltage (kV)	120	120
Inspiratory (mAs)	200	200
Expiratory (mAs)	50	50
Thickness (mm)	0.75	0.75
Interval (mm)	0.5	0.5
Acquisition matrix	512×512	512×512

CT, computed tomography.

size of each patient was dramatically reduced to 2×512×512 from volumetric double-phase CT images, which helps to accelerate model training and testing.

In processing of the clinical information, sex, cough, expectoration, gasp, and wheezing were encoded by means of one-hot encoding. In addition, age, CCQ, and CAT scores were divided into two parts according to their distribution, then each part was encoded using one-hot encoding. Smoking status included never-smokers, ex-smokers, and current smokers; among them, ex-smokers and current smokers were labeled in the same category and never-smokers was labeled other category, then encoded using one-hot encoding. Finally, clinical information was formed into a nine-dimensional vector, which used as input for model in the form of text.

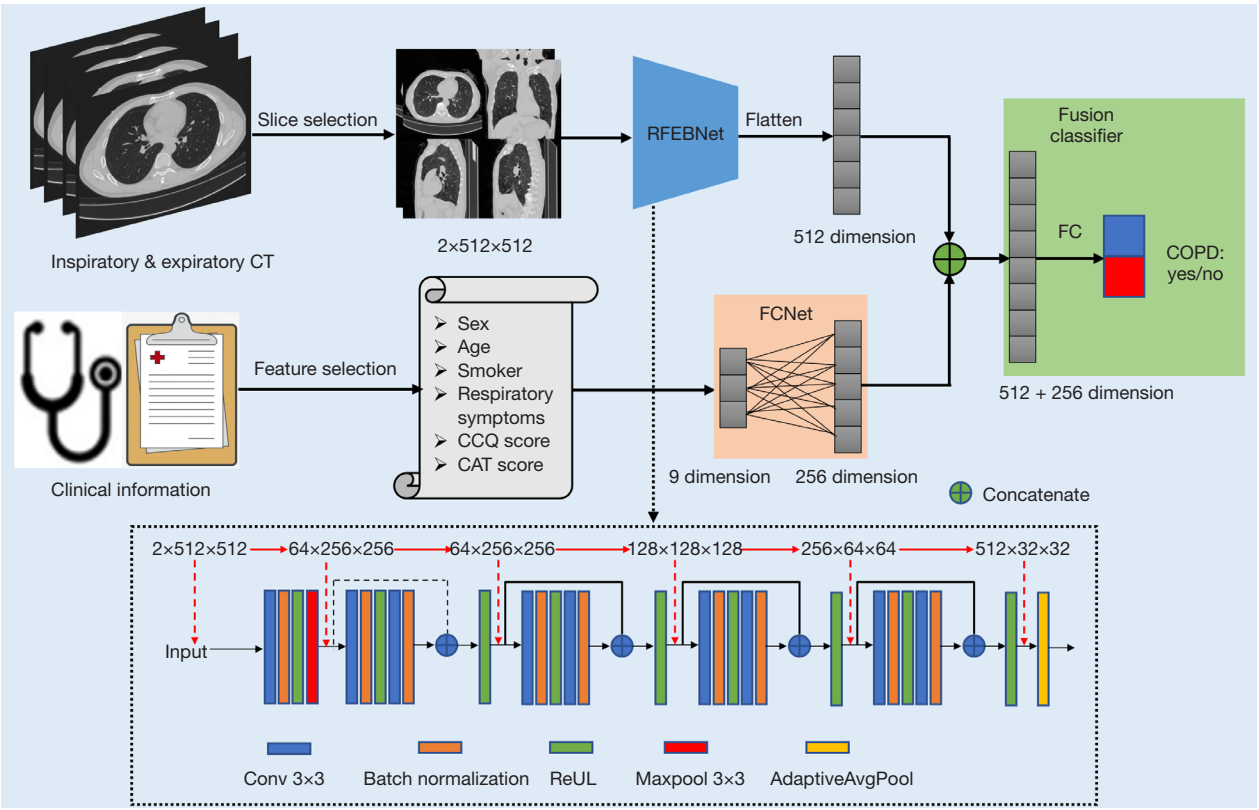

Figure 2 The proposed network architecture for COPD classification. The architecture includes three parts, i.e., a sequence of RFEBNet, a FCNet, and a fusion classifier. RFEBNet is used as an image feature extractor. FCNet is used as a text information extractor. Extracted features from images and clinical information are fed into the fusion classifier for determining COPD or Non-COPD. CT, computed tomography; RFEBNet, residual feature extracting blocks network; FC, fully connected; COPD, chronic obstructive pulmonary disease; CCQ, clinical COPD questionnaire; CAT, COPD assessment test; FCNet, fully connected feed-forward network; ReLU, rectified linear unit.

Model development

Figure 2 shows the architecture of the proposed CNN model. The model includes image feature extractor, text feature extractor, and fusion classifier. The image feature extractor is a sequence of residual feature extracting blocks network (RFEBNet), which is used to extract image features from the selected slices of double-phase CT. Details of RFEBNet are shown in the bottom of *Figure 2*. The first block of RFEBNet consists of a two-dimensional convolutional layer with 64 filtering kernels of size 3×3, batch normalization, rectified linear unit (ReLU) activation function, and a Maxpool, namely, Conv layer→BN layer→ReLU layer→Maxpool layer. After the first block, the input images with size 2×512×512 are transformed into feature maps with size of 64×256×256 (21-23). Then, the feature maps are further fed into a sequence of residual feature extracting blocks (RFEBs). Every RFEB consists of the following structure: Conv layer→BN layer→ReLU layer→Conv layer→BN layer→ReLU layer. In addition, a shortcut path is established to sum the input before the first Conv layer in each RFEB before performing the second ReLU layer. Four RFEB's Conv layer use 64 filtering kernels of size 3×3, 128 filtering kernels of size 3×3, 256 filtering kernels of size 3×3, and 512 filtering kernels of size 3×3, separately. As a result, the size of feature maps is 512×32×32 along the RFEBs. Subsequently, the feature maps obtained from the last RFEB are put into an AdaptiveAvgPool layer to reduce the feature maps size as 512×1×1. Finally, the feature maps are then flattened to a 512-dimensional feature vector. The text feature extractor is a fully connected feed-forward network (FCNet), which is used to extract text features from the corresponding clinical information. The FCNet contains one fully connected (FC) layer. Specifically, the extracted

Table 3 Internal test performance of different models on detecting COPD using parts of Dataset A (n=307)

Model	Model C	Model I	Model E	Model I + E	Proposed
AUC	0.805 (0.777, 0.841)	0.888 (0.863, 0.915)	0.897 (0.874, 0.925)	0.912 (0.891, 0.932)	0.930 (0.913, 0.951)
Sensitivity	0.769 (0.676, 0.842)	0.667 (0.569, 0.753)	0.787 (0.696, 0.858)	0.824 (0.736, 0.889)	0.833 (0.747, 0.896)
Specificity	0.709 (0.640, 0.770)	0.900 (0.847, 0.936)	0.869 (0.813, 0.911)	0.879 (0.824, 0.920)	0.905 (0.853, 0.940)
PPV	0.589 (0.503, 0.670)	0.783 (0.682, 0.859)	0.766 (0.674, 0.839)	0.788 (0.699, 0.857)	0.826 (0.739, 0.889)
NPV	0.849 (0.784, 0.898)	0.833 (0.774, 0.879)	0.883 (0.827, 0.923)	0.902 (0.850, 0.938)	0.910 (0.858, 0.944)
F1-score	0.667 (0.595, 0.738)	0.720 (0.642, 0.798)	0.776 (0.706, 0.847)	0.805 (0.738, 0.873)	0.829 (0.764, 0.895)

Dataset A contains all participants from two of the three hospitals. Data in parentheses are 95% confidence intervals. Model C: a fully connected neural network using clinical information as input; Model I: a sequence of residual feature extracting blocks network using inspiratory chest CT image as input; Model E: a sequence of residual feature extracting blocks network using expiratory chest CT image as input; Model I + E: a sequence of residual feature extracting blocks network using double-phase chest CT images as inputs. COPD, chronic obstructive pulmonary disease; AUC, area under the receiver operating characteristic curve; PPV, positive predictive value; NPV, negative predictive value; CT, computed tomography.

nine-dimensional clinical text vector is encoded by the FC layer into 256-dimensional feature vector. After these two extractors, the 512-dimensional image feature vector and 256-dimensional text feature vector were concatenated and inputted into the fusion classifier for COPD and non-COPD classification.

To evaluate the performance of our proposed CNN model, four neural networks, namely, Model I: RFEBNet using inspiratory chest image as input; Model E: RFEBNet using expiratory chest CT image as input; Model I + E: RFEBNet using double-phase chest CT image as input; and Model C: FCNet using clinical information as input, were also performed for comparison.

Model training

In the training process, training samples were augmented online by random rotation of −30° to 30°, and flipping horizontally and vertically to improve network robustness. The model training parameters were set as follows. The number of epochs was set to 100. The initial learning rate was set to 0.0001 and decayed by five times at each 30 epochs. The batch size was set to eight and weight decay set to 0.001. The Adaptive Movement Estimation (Adam) algorithm was used to optimize the model. All models were implemented with Pytorch framework on a workstation equipped with an NVIDIA RTX A6000 GPU (NVIDIA, Santa Clara, CA, USA) with 48 GB memory capacity.

Model evaluation

To evaluate the performance of the proposed CNN model in detecting COPD, the ROC curve and its 95% confidence interval (CI), AUC, as well as other evaluation metrics including sensitivity, specificity, positive predictive value (PPV), negative predictive value (NPV), and F1-score were calculated. Furthermore, the proposed CNN model's generalizability was evaluated using an external testing set (Dataset B).

Feature extraction visualization

Class activation maps (CAMs) are a visualization technique used to identify which regions of an image contribute the most to a model's classification decision. In the context of the proposed CNN model for COPD detection, CAMs were computed to identify the regions of interest for COPD detection. The CAMs indicate the relative importance of each pixel in the CT image for the classification decision (24).

Statistical analysis

Statistical analysis was conducted using Python version 3.7 and Scikit-learn version 0.24.2 (https://pypi.org/project/scikit-learn/0.24.2/). The 95% CIs were computed using bootstrapping with 1,000 bootstraps. The significance of AUC was tested using the Delong test, and a P value of less than 0.05 was considered statistically significant.

Results

The results of different models in terms of evaluation metrics for diagnosing COPD in the internal test set (n=307) are shown in *Table 3*. Our proposed CNN model,

Table 4 External test performance of different models on detecting COPD using Dataset B (n=516)

Model	Model C	Model I	Model E	Model I + E	Proposed
AUC	0.826 (0.791, 0.865)	0.810 (0.783, 0.845)	0.829 (0.791, 0.865)	0.845 (0.809, 0.886)	0.896 (0.871, 0.931)
Sensitivity	0.856 (0.815, 0.890)	0.818 (0.774, 0.856)	0.889 (0.851, 0.918)	0.924 (0.891, 0.948)	0.905 (0.870, 0.932)
Specificity	0.660 (0.577, 0.735)	0.626 (0.542, 0.703)	0.544 (0.460, 0.626)	0.517 (0.433, 0.600)	0.694 (0.612, 0.766)
PPV	0.863 (0.823, 0.896)	0.846 (0.803, 0.881)	0.830 (0.789, 0.865)	0.828 (0.787, 0.862)	0.881 (0.843, 0.911)
NPV	0.647 (0.564, 0.722)	0.579 (0.498, 0.656)	0.661 (0.569, 0.743)	0.731 (0.633, 0.811)	0.744 (0.662, 0.813)
F1-score	0.860 (0.827, 0.893)	0.832 (0.796, 0.868)	0.859 (0.829, 0.891)	0.873 (0.842, 0.904)	0.893 (0.863, 0.923)

Dataset B contains those from the other hospital. Data in parentheses are 95% confidence intervals. Model C: a fully connected neural network using clinical information as input; Model I: a sequence of residual feature extracting blocks network using inspiratory chest CT image as input; Model E: a sequence of residual feature extracting blocks network using expiratory chest CT image as input; Model I + E: a sequence of residual feature extracting blocks network using double-phase chest CT images as inputs. COPD, chronic obstructive pulmonary disease; AUC, area under the receiver operating characteristic curve; PPV, positive predictive value; NPV, negative predictive value; CT, computed tomography.

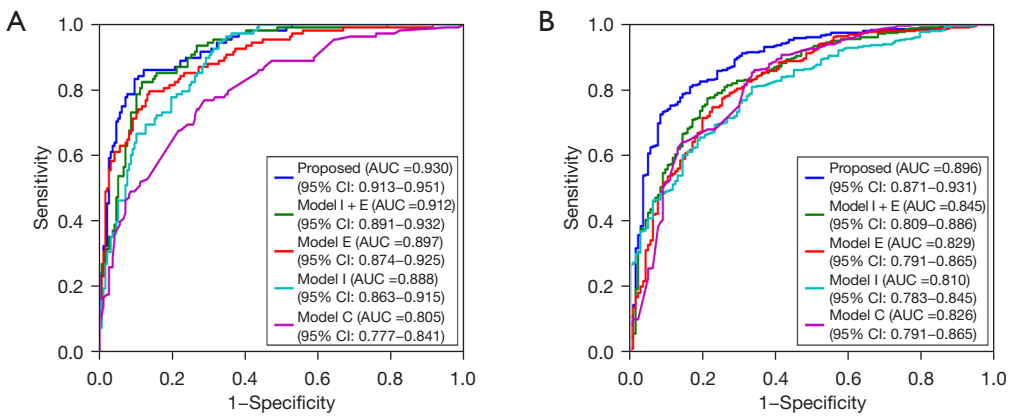

Figure 3 ROC curve comparison between different models in the internal (A) and external (B) tests, respectively. Model I + E: a sequence of residual feature extracting blocks network using double-phase chest CT images as inputs; Model E: a sequence of residual feature extracting blocks network using expiratory chest CT image as input; Model I: a sequence of residual feature extracting blocks network using inspiratory chest CT image as input; Model C: a fully connected neural network using clinical information as input. ROC, receiver operating characteristic; AUC, area under the receiver operating characteristic curve; CI, confidence interval; CT, computed tomography.

by combining double-phase CT and clinical information, achieved the best classification performance on detecting COPD with an AUC of 0.930, sensitivity of 0.833, specificity of 0.905, PPV of 0.826, NPV of 0.910, and F1-score of 0.829. In contrast, Model C, which was based on FCNet using clinical information only, had the worst classification performance with an AUC of 0.805, sensitivity of 0.769, specificity of 0.709, PPV of 0.589, NPV of 0.849, and F1-score of 0.667. Model I + E, which was based on RFEBNet using inspiratory and expiratory CT, had an AUC of 0.912, sensitivity of 0.824, specificity of 0.879, PPV of 0.788, NPV of 0.902, and F1-score of 0.805. It had better performance than Model I (based on RFEBNet using inspiratory only) and Model E (based on RFEBNet using expiratory CT only) in terms of AUC (0.912 *vs.* 0.888, P value <0.001 and 0.912 *vs.* 0.897, P value =0.042, respectively).

The external test set had similar results with the internal test set (*Table 4*). The proposed model also achieved the highest evaluating metrics in terms of AUC, specificity, PPV, NPV, and F1-score, except that the sensitivity was slightly lower than that of Model I + E. The corresponding ROC curve comparison of the different models in the internal and external test set are shown in *Figure 3*.

As depicted in *Figure 4*, the proposed model exhibited

A

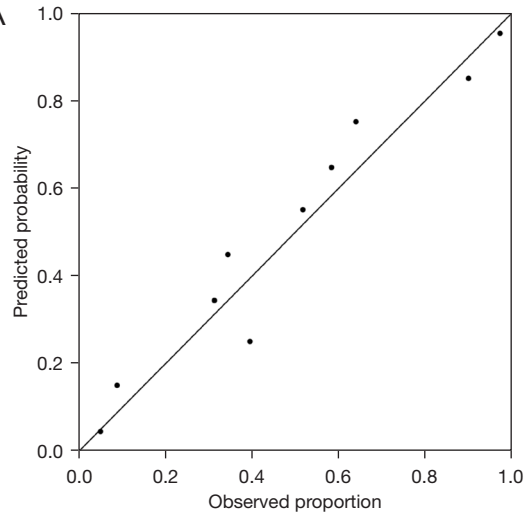

B

COPD classification by decile of predicted probability	
Observed proportion with clinical COPD	Predicted probability of COPD
0.05	0.0423
0.09	0.1512
0.32	0.3456
0.36	0.4525
0.40	0.2545
0.51	0.5432
0.60	0.6714
0.63	0.7532
0.90	0.8723
0.96	0.9516

Hosme-Lemeshow P>0.99

Figure 4 Detection of COPD by the proposed model in the internal test set. (A) The predicted probabilities represent the predicted probability that the proposed model assigns to the outcome of COPD. The observed proportions reflect the actual proportion of participants within each decile who were diagnosed with COPD. Reference lines illustrate perfect correlation, with a slope of 1 and an intercept of 0. (B) The Hosmer-Lemeshow test assessed as calibration quality. A nonsignificant P value (>0.05) suggests that there is no evidence for poor calibration. COPD, chronic obstructive pulmonary disease.

excellent calibration for COPD detection, as indicated by the Hosmer-Lemeshow test (P>0.99), suggesting no evidence of poor calibration. *Figure 5* presents several examples of original inspiratory CT images and their corresponding saliency maps between COPD and non-COPD, which were obtained by our proposed model. Saliency maps display regions of an image that are most relevant to a model's decision-making process, with hotter colors indicating higher importance. The information derived from saliency maps suggests that the proposed model focuses on areas around the lung and some rib margin. As shown in *Figure 5*, most of the regions in the non-COPD lung were blue (*Figure 5E,5F*), whereas many hot colors appeared in the COPD lung and some rib margins (*Figure 5A-5D*).

Discussion

In this study, we developed a novel CNN model that integrates double-phase CT images and clinical information to improve the accuracy of COPD detection. It achieved the highest AUC in the internal test set, and its generalizability was validated by the external test set.

The proposed model demonstrated superior performance in COPD detection. One of the key factors contributing to the model's success is the use of double-phase CT images. This allows for capturing more features on identifying COPD. For example, the air-trapping is a potential early symptom of COPD that can only be observed on expiratory CT images (14). Another critical component is that we implemented model concatenation, not only extracting images features but also incorporating clinical information. This multivariate model is more in line with clinical diagnosis practice. Therefore, by merging this clinical information with the double-phase CT images, the proposed model was better equipped to identify COPD.

This study has significant implications for clinical practice in detecting COPD. The Model E using expiratory CT images had better performance in many evaluation indicators compared to the Model I using inspiratory CT images. This suggests that expiratory CT may provide more useful COPD features for detection than inspiratory CT. This finding emphasizes the importance of considering the role of expiratory CT in COPD detection in clinical practice. Another strength of this study is the inclusion of a well-representative population of over 2,000 patients from three hospitals, including never-smokers, ex-smokers, and current smokers undergoing COPD screening. These findings may have important implications for the development of future screening and diagnostic approaches for COPD.

Nevertheless, our study had two limitations. Firstly, obtaining additional expiratory CT images increased the

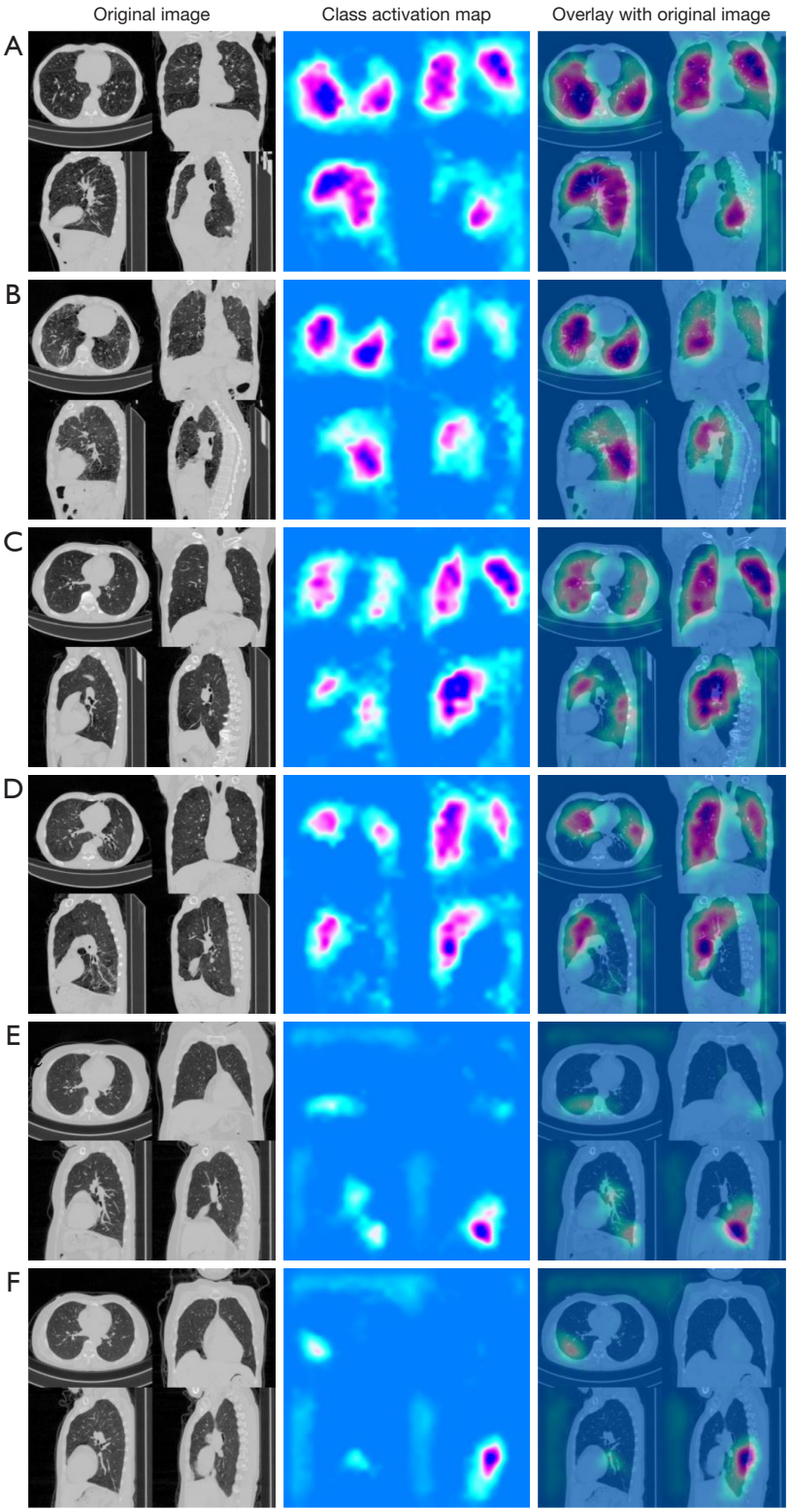

Figure 5 Feature visualizations of proposed model for detecting COPD using CAMs technique. The columns from left to right are the original inspiratory CT image, a class activation map, and a class activation map overlaying the original image. (A-D) COPD cases. (E,F) Non-COPD cases. COPD, chronic obstructive pulmonary disease; CAMs, class activation maps; CT, computed tomography.

radiation dose to the patient, whereas this study aimed to evaluate the utility of expiratory CT imaging for COPD detection and did not focus on the potential risks associated with increased radiation exposure. Secondly, compared with obtaining inspiratory CT images, it is more difficult to obtain true expiratory CT images from patients, particularly those with shortness of breath.

Conclusions

The proposed CNN model, which fully utilizes the information from double-phase CT images and clinical data, has demonstrated the ability to improve the accuracy of COPD detection. Our findings suggest that the proposed model has the potential to be used as an automatic screening tool for identifying COPD patients in clinical practice.

Acknowledgments

The authors thank all the participants who participated in this study.
Funding: This study was supported by the Foundation of Guangzhou National Laboratory (Nos. SRPG22-016 and SRPG22-018), the Clinical and Epidemiological Research Project of State Key Laboratory of Respiratory Disease (No. SKLRD-L-202402), the Plan on Enhancing Scientific Research in Guangzhou Medical University (No. GMUCR2024-01012), and the Key Scientific Research Project of Universities in Guangdong Province (No. 2023KCXTD026).

Footnote

Reporting Checklist: The authors have completed the TRIPOD reporting checklist. Available at https://jtd.amegroups.com/article/view/10.21037/jtd-24-367/rc

Data Sharing Statement: Available at https://jtd.amegroups.com/article/view/10.21037/jtd-24-367/dss

Peer Review File: Available at https://jtd.amegroups.com/article/view/10.21037/jtd-24-367/prf

Conflicts of Interest: All authors have completed the ICMJE uniform disclosure form (available at https://jtd.amegroups.com/article/view/10.21037/jtd-24-367/coif). The authors have no conflicts of interest to declare.

Ethical Statement: The authors are accountable for all aspects of the work in ensuring that questions related to the accuracy or integrity of any part of the work are appropriately investigated and resolved. The study was conducted in accordance with the Declaration of Helsinki (as revised in 2013). The study was approved by the Ethics Committee of Scientific Research Project Review of The First Affiliated Hospital of Guangzhou Medical University (No. 2018-53) and informed consent was provided by all individual participants.

References

1. Vogelmeier CF, Criner GJ, Martinez FJ, et al. Global Strategy for the Diagnosis, Management, and Prevention of Chronic Obstructive Lung Disease 2017 Report. GOLD Executive Summary. Am J Respir Crit Care Med 2017;195:557-82.
2. Prevalence and attributable health burden of chronic respiratory diseases, 1990-2017: a systematic analysis for the Global Burden of Disease Study 2017. Lancet Respir Med 2020;8:585-96.
3. Bellamy D, Smith J. Role of primary care in early diagnosis and effective management of COPD. Int J Clin Pract 2007;61:1380-9.
4. Tammemagi MC, Schmidt H, Martel S, et al. Participant selection for lung cancer screening by risk modelling (the Pan-Canadian Early Detection of Lung Cancer [PanCan] study): a single-arm, prospective study. Lancet Oncol 2017;18:1523-31.
5. de Koning HJ, van der Aalst CM, de Jong PA, et al. Reduced Lung-Cancer Mortality with Volume CT Screening in a Randomized Trial. N Engl J Med 2020;382:503-13.
6. Mets OM, Buckens CF, Zanen P, et al. Identification of chronic obstructive pulmonary disease in lung cancer screening computed tomographic scans. JAMA

2011;306:1775-81.
7. González G, Ash SY, Vegas-Sánchez-Ferrero G, et al. Disease Staging and Prognosis in Smokers Using Deep Learning in Chest Computed Tomography. Am J Respir Crit Care Med 2018;197:193-203.
8. Tang LYW, Coxson HO, Lam S, et al. Towards large-scale case-finding: training and validation of residual networks for detection of chronic obstructive pulmonary disease using low-dose CT. Lancet Digit Health 2020;2:e259-67.
9. Ho TT, Kim T, Kim WJ, et al. A 3D-CNN model with CT-based parametric response mapping for classifying COPD subjects. Sci Rep 2021;11:34.
10. Sun J, Liao X, Yan Y, et al. Detection and staging of chronic obstructive pulmonary disease using a computed tomography-based weakly supervised deep learning approach. Eur Radiol 2022;32:5319-29.
11. Xu C, Qi S, Feng J, et al. DCT-MIL: Deep CNN transferred multiple instance learning for COPD identification using CT images. Phys Med Biol 2020;65:145011.
12. Wu Y, Du R, Feng J, et al. Deep CNN for COPD identification by Multi-View snapshot integration of 3D airway tree and lung field. Biomedical Signal Processing and Control 2023;79:104162.
13. Du R, Qi S, Feng J, et al. Identification of COPD From Multi-View Snapshots of 3D Lung Airway Tree via Deep CNN. IEEE Access 2020;8:38907-19.
14. Labaki WW, Martinez CH, Martinez FJ, et al. The Role of Chest Computed Tomography in the Evaluation and Management of the Patient with Chronic Obstructive Pulmonary Disease. Am J Respir Crit Care Med 2017;196:1372-9.
15. Gawlitza J, Trinkmann F, Scheffel H, et al. Time to Exhale: Additional Value of Expiratory Chest CT in Chronic Obstructive Pulmonary Disease. Can Respir J 2018;2018:9493504.
16. Hasenstab KA, Yuan N, Retson T, et al. Automated CT Staging of Chronic Obstructive Pulmonary Disease Severity for Predicting Disease Progression and Mortality with a Deep Learning Convolutional Neural Network. Radiol Cardiothorac Imaging 2021;3:e200477.
17. Jones PW, Harding G, Berry P, et al. Development and first validation of the COPD Assessment Test. Eur Respir J 2009;34:648-54.
18. van der Molen T, Willemse BW, Schokker S, et al. Development, validity and responsiveness of the Clinical COPD Questionnaire. Health Qual Life Outcomes 2003;1:13.
19. González G, Washko GR, Estépar RS. Automated Agatston score computation in a large dataset of non ECG-gated chest computed tomography. Proc IEEE Int Symp Biomed Imaging 2016;2016:53-7.
20. Zhou RG, Hu W, Fan P, et al. Quantum realization of the bilinear interpolation method for NEQR. Sci Rep 2017;7:2511.
21. He K, Zhang X, Ren S, et al. Deep Residual Learning for Image Recognition. 2016 IEEE Conference on Computer Vision and Pattern Recognition (CVPR). Las Vegas, NV, USA: IEEE; 2016:770-8.
22. Ioffe S, Szegedy C. Batch Normalization: Accelerating Deep Network Training by Reducing Internal Covariate Shift. PMLR 2015;37:448-56.
23. Eckle K, Schmidt-Hieber J. A comparison of deep networks with ReLU activation function and linear spline-type methods. Neural Netw 2019;110:232-42.
24. Kwaśniewska A, Rumiński J, Rad P. Deep features class activation map for thermal face detection and tracking. 2017 10th International Conference on Human System Interactions (HSI). Ulsan: IEEE; 2017:41-7.

Cite this article as: Zhang Z, Wu F, Zhou Y, Yu D, Sun C, Xiong X, Situ Z, Liu Z, Gu A, Huang X, Zheng Y, Deng Z, Zhao N, Rong Z, He J, Xie G, Ran P. Detection of chronic obstructive pulmonary disease with deep learning using inspiratory and expiratory chest computed tomography and clinical information. J Thorac Dis 2024;16(9):6101-6111. doi: 10.21037/jtd-24-367